ACS APPLIED MATERIALS & INTERFACES

RESEARCH ARTICLE

www.acsami.org

Vertically Aligned Single-Walled Carbon Nanotubes as Low-cost and High Electrocatalytic Counter Electrode for Dye-Sensitized Solar Cells

Pei Dong,[†] Cary L. Pint,[‡] Mel Hainey,[†] Francesca Mirri,[§] Yongjie Zhan,[†] Jing Zhang,[⊥] Matteo Pasquali,[§] Robert H. Hauge,[‡] Rafael Verduzco,[§] Mian Jiang,[#] Hong Lin,[*,⊥] and Jun Lou[*,†]

[†]Mechanical Engineering and Materials Science, [‡]The Richard E. Smalley Institute for Nanoscale Science and Technology, and [§]Department of Chemical and Biomolecular Engineering, Rice University, 6100 Main, Houston, Texas 77005, United States

[⊥]Department of Materials Science and Engineering, Tsinghua University, Beijing 100084, P. R. China

[#]Department of Natural Sciences, University of Houston Downtown, One Main Street, Houston, Texas 77002, United States

Supporting Information

ABSTRACT: A novel dye-sensitized solar cell (DSSC) structure using vertically aligned single-walled carbon nanotubes (VASWCNTs) as the counter electrode has been developed. In this design, the VASWCNTs serve as a stable high surface area and highly active electrocatalytic counter-electrode that could be a promising alternative to the conventional Pt analogue. Utilizing a scalable dry transfer approach to form a VASWCNTs conductive electrode, the DSSCs with various lengths of VASWCNTs were studied. VASWCNTs-DSSC with 34 μm original length was found to be the optimal choice in the present study. The highest conversion efficiencies of VASWCNTs-DSSC achieved 5.5%, which rivals that of the reference Pt DSSC. From the electrochemical impedance spectroscopy analysis, it shows that the new DSSC offers lower interface resistance between the electrolyte and the counter electrode. This reproducible work emphasizes the promise of VASWCNTs as efficient and stable counter electrode materials in DSSC device design, especially taking into account the low-cost merit of this promising material.

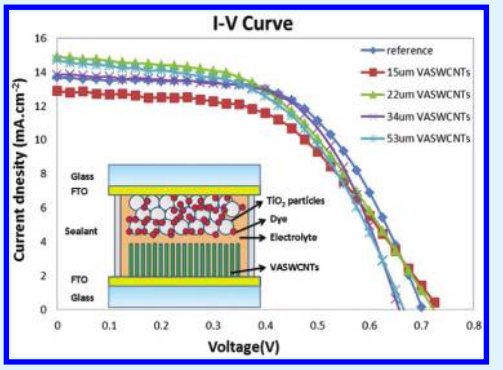

KEYWORDS: dye-sensitized solar cells, vertically aligned single-walled carbon nanotubes, counter electrodes, electrocatalytic activity

1. INTRODUCTION

Dye-sensitized solar cells (DSSCs) are a relatively new class of thin film solar cells with promising high conversion efficiency at a low cost. These solar cells utilize two main components: a photo anode consisting of light-absorbing dye molecules adsorbed on a semiconductor material, and an electrically conductive counter electrode that catalyzes an electrolyte redox reaction to regenerate electrons for the dye molecules.[1−5] Because these cells do not utilize highly processed silicon for light harvesting, they may be fabricated at much lower cost than traditional photovoltaic cells. In this device, the counter electrode material choice is one of the key factors in achieving a highly efficient DSSC device. A Pt thin film deposited on a fluorine doped tin oxide (FTO) substrate typically serves as the counter electrode in conventional DSSCs.[6−8] While offering excellent electrical conductivity, catalytic activity, and corrosion resistance, Pt is also an expensive and relatively rare element. To lower materials cost and achieve feasible large-scale production, an alternative counter electrode material with excellent high conductivity as well as superior electrocatalytic activity is highly desirable. Because of the low cost, high durability, excellent catalytic activity, and electrical conductivity, carbon-based materials have been utilized as effective alternative counter electrode for many years.[4,9−11] Carbon nanotubes and nanohorns,[4] carbon black,[10] and graphite[11] have all been tested as potential counter electrodes. Traditionally, these structures have been applied as 2D films, but this approach suffers several drawbacks. The 2D structure limits the available catalytic surface area of the carbon material, and electron transfer is less efficient because the electrons must hop between the different carbon structures within the film during transport. Vertically aligned carbon nanotubes (VACNTs) present a solution to both of these problems. Stemming from the high surface to volume ratio of VACNTs', this 3D structure has much higher available catalytic surface area than any 2D film, and its vertical alignment allows direct electron transport to occur through individual tubes, which will eliminate the contact resistance encountered in 2D counter electrodes. Proving the validity of this approach, a DSSC utilizing vertically-aligned multi-walled carbon nanotubes (VAMWCNTs) counter electrode was fabricated by J. G. Nam et al. and it was found that the vertical alignment realized by low temperature chemical vapor deposition (CVD) growth of VAMWCNTs directly on FTO glass clearly improved the fill factor (FF) thus corresponding cell efficiency

Received: May 23, 2011
Accepted: July 19, 2011
Published: July 19, 2011

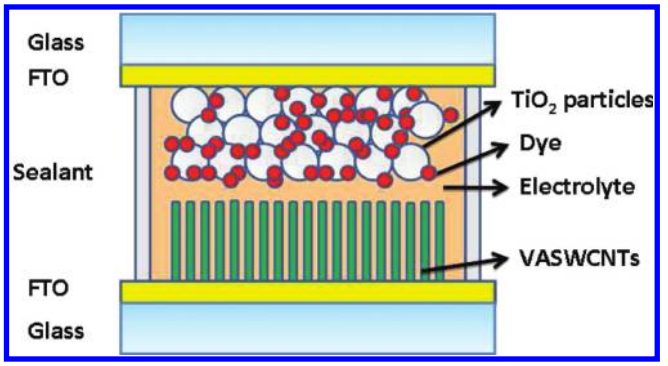

Figure 1. Schematic of VASWCNTs-DSSC.

as compared to the deposited 2D MWNT films.[4] Lee et al.[5] and Ramasamy et al.[12] further proved the efficiency was related to the thickness of MWCNT as a result of variations in the charge transfer resistance between the electrolyte and carbon nanotubes (CNTs) interface.

Single-walled carbon nanotubes (SWCNTs) have smaller diameters than multi-walled nanotubes while offering comparable or better electrical and catalytic properties. Vertically aligned SWCNTs (VASWCNTs) therefore could provide even higher catalytic surface areas than VAMWCNTs arrays, and have the potential to offer superior catalytic performance.

In this spirit, dense VASWCNTs is an ideal material to be utilized as a counter electrode due to their attractive features — combining a high surface area counter electrode that is chemically stable, with excellent electrical transport properties due to the one-dimensional nature of the SWCNTs. Due to these reasons, there have been a few reports of using SWCNTs as counter electrodes in DSSC devices. Suzuki et al. reported on the casting of SWCNTs films on FTO-glass and Teflon membranes to make counter-electrodes for DSSCs, demonstrating conversion efficiencies of 3.5 and 4.5%, respectively,[13] which was still appreciably lower than that of traditional Pt based DSC (5.4%). In 2009, Lee et al. achieved 4.03% conversion efficiency from adding SWCNTs to Pt as the counter anode.[14] In 2010, an efficiency of around 8% by using gel-coated binder-free SWCNTs were reported.[15] In the same year, C. Wang's group achieved 1.3037% by employing SWCNTs with functional group deposition.[16] SWCNTs had also been applied on different substrates in DSSC, i.e., stainless steel[17] and flexible PET substrates.[18] All of the above had used wet processing methods which involve dispersing SWCNTs in solvents then spraying or spin coating the solution onto substrates to prepare the SWCNTs counter electrode. Nonetheless, there remains significant variation between the conversion efficiencies reported using different counter electrode preparation approaches, making it difficult to assess the promise of SWCNTs as a counter electrode material for DSSCs.

In this study, we employed high quality VASWCNTs arrays as counter electrodes for DSSC device design, demonstrating the use of a dry-transfer of the SWCNT arrays to produce robust counter electrodes on FTO-glass substrates (Figure 1). Compared with wet processing methods, the dry method is simple, repeatable and easy to control, offering high density of SWCNTs arrays. Using this scalable counter electrode fabrication approach, the conversion efficiencies of 5.5% were obtained, yielding a competitive counter electrode design to the expensive Pt electrode. Also we studied the DSSC with various lengths of VASWCNTs as counter electrode. It turned out that VASWCNTs with ~34 μm original length produced the best result. On the basis of this study, we expect an optimized SWCNT material to be an ideal candidate for low-cost, scalable, and highly efficient DSSC device design in the future.

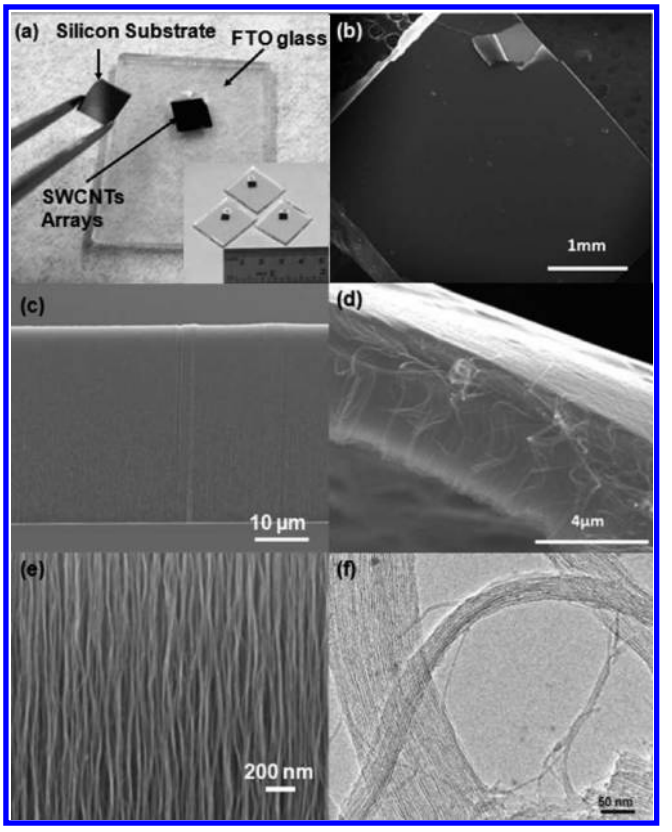

Figure 2. Characteristics of a representative VASWCNTs array (a) transfer VASWCNTs from silicon substrate to FTO (inserted picture: three VASWCNTs counter eletrode); (b, c, e) SEM images of VASWCNTs before transfer; (d) SEM image of VASWCNTs after transfer. (f) TEM image of VASWCNTs.

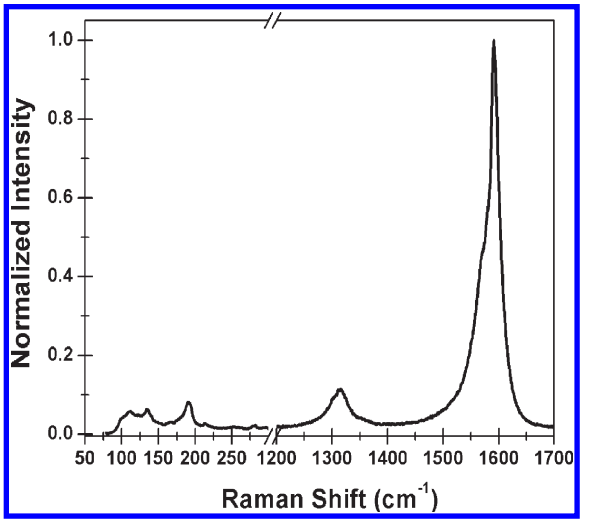

Figure 3. Raman spectra of VASWCNTs.

2. RESULTS AND DISCUSSION

Figure 2a is a picture showing the original growth substrate being held by a tweezers to demonstrate the clean transfer from

Table 1. *I*−*V* Parameters of VASWCNTs-DSSCs

as-grown lengths	after-transfer lengths (μm)	V_{oc} (V)	current density (mA cm^{-2})	FF (%)	efficiency (%)
reference	N/A	0.7	13.67	59	5.6
15 μm VASWCNTs	~1	0.725	12.9	51	4.8
22 μm VASWCNTs	~3	0.725	14.88	49	5.3
34 μm VASWCNTs	~6	0.65	13.8	61	5.5
53 μm VASWCNTs	~7	0.675	14.73	52	5.1

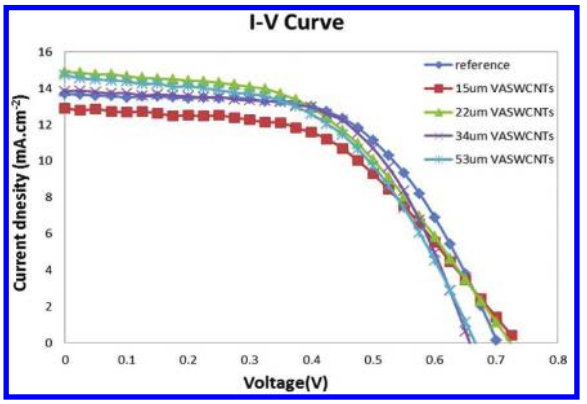

Figure 4. *I*−*V* curves of the reference and the VASWCNTs-DSSCs.

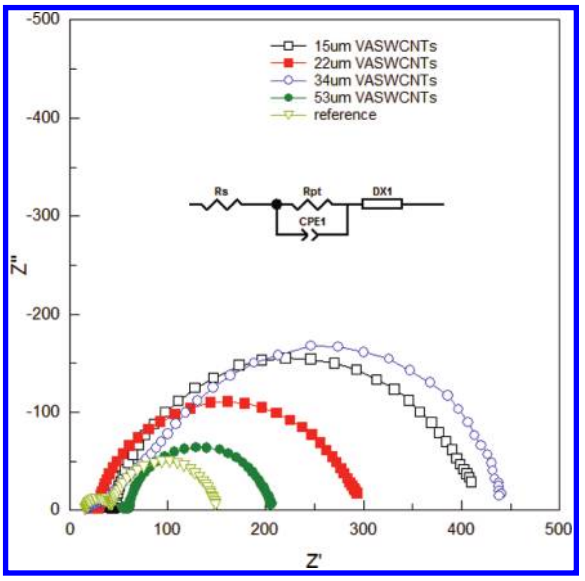

Figure 5. Nyquist plots of the VASWCNTs-DSSCs at different bias voltages.

one surface to the next that was consistently observed in this study. Inset in Figure 2a is an image of SWCNTs arrays transferred to FTO-glass substrates prior to fabricating DSSC devices. The area of the fabricated VASWCNTs counter electrode used in our DSSC devices is typically ~0.11 cm^2. Detailed, systematic studies of the effect of SWCNTs array length suggested optimal device performance at lengths of ~34 μm, prior to transfer of the VASWCNTs. The characteristics of a representative SWCNT array, including scanning electron microscopy (SEM, FEI Quanta 400 ESEM, FEI, USA) imaging before (Figure 2b, c, e) and after (Figure 2d) contact transfer to FTO are shown. High-resolution transmission electron microscopy (TEM, JEOL 2010, JEOL, Japan) characterization and Raman spectra are shown in Figures 2f and 3. From the Raman characterization (633 nm excitation), it is evident that the SWCNTs are of high quality, with a G/D ratio ~10 suggesting a very low amount of defects of amorphous carbon in the material. Also observable are some radial breathing modes from the SWCNTs, depicting the wide range of diameters present in the SWCNTs arrays. To characterize the SWCNT material, we imaged as-grown and transferred SWCNT arrays (Table 1). For example, prior to transfer of one of the VASWCNTs arrays, the original lengths (controllably tuned utilizing the known relation between the growth time and the carpet height[19]) were ~34 μm. Following the transfer, the lengths of the SWCNTs array were observed to be ~6 μm due to some compression by an applied shear-force that is placed on the SWCNTs array to facilitate transfer. This compaction effect, although in a varying degree, was consistently observed in all VASWCNTs array transfer processes with different original lengths (Table 1). Typical measured carbon densities of this material are ~60 mg/cm^3,[20] with measured average SWCNTs diameters near 2.5 nm.[21] These are determined utilizing a combination of mass measurements, optical measurements, and electron microscopy. This yields a ~7% dense material following growth. This means that following transfer the structure is, on average, ~40% dense, leading to better conduction properties while still maintaining a high exposed surface area.

Figure 2e depicts a high magnification image of the SWCNT array, showing the bundle structure (average bundle diameter of ~20 nm) and the good alignment in the as-grown SWCNTs array. Figure 2f shows TEM characterization of the SWCNT material, after sonication in ethanol and drop casting onto a TEM grid. Evident from these images are SWCNTs that have a diameter range (2−4 nm) consistent with previous detailed imaging and characterization reported elsewhere.[19,21]

To evaluate the DSSC performance, we tested one group of reference DSSC with Pt used as counter electrode (with the same area as VASWCNTs electrodes) and four groups of VASWCNTs-DSSC with different SWCNT lengths. The characteristic I−V plots of the devices are shown in Fig. 4 and the detailed photovoltaic parameters are summarized in Table 1. For the DSSCs made from VASWCNTs with 34μm original length, the short-circuit current densities (J_{sc}) are measured to be 13.8 mA/cm^2 yielding a total conversion efficiency of 5.5% (SWCNT area of 0.11 cm^2), with an open-circuit voltage (V_{oc}) and FF of 0.66 V and 61%, respectively. Based on Table 1, the efficiency of the DSSC made from VASWCNTs with 34μm original length achieved the highest value, compared with other VASWCNTs-DSSCs. An efficiency of 5.5% is also very close to the efficiency of the reference DSSC fabricated following the same procedure as described earlier but employed evaporated Pt as counter electrode,

which is 5.6%. The difference between 5.5% and 5.6% is negligible, because of the margin of error of estimates that go into the efficiency, such as measuring dimensions of the DSSC device and reasonable offset of the solar simulator. In other words, these two values are the same within the accuracy of the measurement technique.

To further understand the important parameters in the operation of the DSSCs, the electrochemical impedance spectroscopy (EIS) analysis employing the ZView software were carefully conducted. As clearly shown in Figure 5, there are two semi-circles in the Nyquist plots. After we fit the plots with the equivalent circuit (insert in Figure 5, where CPE 1 = Constant Phase Element #1; DX 1= Extended Distributed Elements #1), the charge transfer resistance (Rpt) of VASWCNTs was found to be from 5Ω to 10Ω, depends on their different lengths; while the Rpt of the reference DSSC was around 30Ω. This proves that the VASWCNTs offer lower interface resistance between the electrolyte and counter electrode, compared to the reference DSSC.

At the same time, the series resistance (Rs) of VASWCNTs-DSSC is from 18 to 49 Ω depends on different lengths, while Rs of the reference DSSC is around 16 Ω. The intrinsic resistance of the VASWCNTs have been measured (along their length) to be near $\sim 3 \times 10^{-6}$ Ωm,[22,23] which should yield a significantly lower resistance than 18 to 49 Ω. Because the resistance of FTO is the same in both VASWCNTs-DSSCs and the reference DSSC, it can be assumed that the high resistance is directly related to the mechanical contact between the VASWCNTs and FTO glass which could be further improved. However, it is notable that even with this non-ideal condition, the DSSC devices fabricated in this way still achieved 5.5% conversion efficiency, which is almost the same to 5.6% in the reference DSSC, within the margin of error.

Meanwhile, important parameters including recombination impedance and chemical capacitance were also analyzed for both VASWCNTs-DSSCs and the reference DSSC, demonstrating a non-negligible effect of VASWCNTs electrodes on photo anode performances (see the Supporting Information). Furthermore, measurement of monochromatic incident photon-to-electron conversion efficiency (IPCE) of VASWCNTs-DSSCs confirmed the sub-optimal performances of photo anodes (see the Supporting Information), suggesting the possibilities of increasing the total conversion efficiency by improving the quality of photo electrodes.

Finally, it should be noted that a key advance in this study is the integration of high quality VASWCNTs into the DSSC device design. In this architecture, the ultra-long VASWCNTs arrays (as shown in Figure 2c) allows direct contacts between electrolyte and the FTO surfaces that is mediated by individual SWCNT assembled in parallel. This allows charge transport processes to be determined by intra-tube transport, as opposed to inefficient electron hopping processes that occur between nanotubes[22] and are likely to limit the performance of CNTs electrodes prepared utilizing other techniques.

Therefore, the scheme developed in the current study made it possible for the electrical resistance of the high surface area electrode material to be significantly reduced, while also providing a technique promising for scalable and cost-effective counter electrode fabrication for DSSC devices. These results suggest that VASWCNTs could eventually yield better performance compared to Pt as a counter electrode material in DSSC device design.

3. CONCLUSIONS

In conclusion, we explored the performance of VASWCNTs-DSSCs with various SWCNT lengths. This DSSC architecture with ~34μm VASWCNTs length was found to yield the optimal counter electrode in our systematic study. Our experiments determine that the VASWCNTs-DSSC has an efficiency of 5.5%, comparable to 5.6% obtained with a reference Pt-DSSC. EIS measurements determine that the electrolyte-VASWCNTs resistance in this architecture is lowered by up to ~6× compared to Pt, whereas the VASWCNTs-FTO interface has a higher resistance due to the contact transfer process utilized here. Nonetheless, our studies emphasize that future work focus on improving the electrical interface between VASWCNTs arrays and the back-contact could yield DSSC device performance exceeding that which can be obtained with a traditional counter electrode design, while also providing a lower-cost alternative to Pt.

4. METHODS

To fabricate VASWCNTs-DSSC devices, the VASWCNTs were grown in a water-assisted thermal chemical vapor deposition system at 750 °C utilizing atomic hydrogen catalyst reduction prior to growth.[13] The catalyst substrates consisted of 0.5 nm thick Fe films and subsequent 10 nm thick Al_2O_3 films deposited onto Si. Following growth, the carbonaceous interface between the catalyst and the SWCNTs was etched using a 3−5 min vapor phase H_2/H_2O treatment at 750 °C, and the SWCNT arrays were transferred by simple contact printing in a manner described in detail elsewhere.[21,24] In brief, the VASWCNTs morphology enables strong van Der Waals interfacial adhesion with a surface that it is placed in contact with compared to the interaction with the growth substrate (where this interface has been etched). This allows simple contact transfer in the framework of the "gecko effect" that is performed in a fully dry state, and allows the VASWCNTs material to be transferred to nearly any surface. This technique leaves the metal catalyst behind on the growth substrate whereas the transferred SWCNTs are clean and free of metal impurities. Evidence of this is clear in studies where aligned SWCNTs are grown multiple times following contact transfer from the same 0.5 nm thick catalyst layer.[25] As a result of its simplicity, this technique is highly scalable and could be envisioned to take place in a roll-to-roll, or large-scale industrial process, as such techniques are currently being developed.[26] Following transfer, this counter electrode is assembled into a modified DSSC architecture, as illustrated in Figure 1. Finally for the fabrication of Pt reference electrodes, a CRC-150 sputter coater was utilized to sputter Pt thin films with thickness of 20 nm and an average RMS value of a few nm on FTO substrates.

The FTO glasses (Pilkington FTO glass Tec 8 &15 Glass, 2.2 mm of thickness) were cleaned using an ultrasonic bath in a detergent solution, consisting of DI water and 200 proof alcohol, and repeated twice. The clean FTO glasses were screen-printed with TiO_2 paste. The paste for the transparent TiO_2 layer (DSL 18NR-T, Dyesol) was printed four times on the FTO glass plate. A diffusing layer (WER4-O, Dyesol) was then formed once. The printed thickness was controlled to 12.5 μm by successive printing. After each printing, each layer was dried at 125 °C for 6 minutes and then sintered at 500 °C for 60 min in air. Anatase structure was confirmed from the X-ray diffraction (XRD) result. The sintered photo electrode was immersed in the N719 (Ruthenium, $RuL_2(NCS)_2$): 2 TBA (L = 2,2′-bipyridyl-4,4′-dicarboxylic acid; TBA = tetra-*n*-butylammonium), B2 N719, Dyesol) solution (3×10^{-4} mol/L) for 24 h at room temperature.

The photo electrode and counter electrode were stacked and sealed with a sealant (1170 Series, 25 and 60μm, Solaronix) at 125 °C for 20 s twice. The electrolyte solution, with a composition of 50 mM I_2, 500 mM LiI, 500 mM 4-tert-butylpyridine (TBP), and 2-methoxypropionitrile (MPN) as the solvent, was injected into the cell and sealed using additional sealant.

To characterize the performance of DSSC devices with VASWCNTs as the counter-electrode material, we performed testing under standard

conditions (AM 1.5, 100 mW/cm^2) at 25 °C using a solar simulator (Oriel) calibrated using a reference silicon cell (calibrated at NREL, Oriel). Electrical impedance measurements were tested using a 608C electrochemical analyzer workstation (CH Instruments, Austin, Texas). The frequency range is from 0.05 Hz to 100,000 Hz, while the magnitude of the modulation signal is 5 mV. Z-View software (v2.9c, Scribner Associates Inc.) was utilized to fit the experimentally measured spectra with the appropriate equivalent circuit.

■ ASSOCIATED CONTENT

Supporting Information. Four figures, including a semi logarithmic plot of the recombination impedance (R_{ct}), a semi logarithmic plot of the chemical capacitance ($C\mu$), a plot of the apparent electron lifetime (τn) and the monochromatic incident photon-to-electron conversion efficiency (IPCE) of VASWCNTs-DSSC. This material is available free of charge via the Internet at http://pubs.acs.org.

■ AUTHOR INFORMATION

Corresponding Author
*E-mail: hong-lin@tsinghua.edu.cn (H.L.); jlou@rice.edu (J.L.).

■ ACKNOWLEDGMENT

The authors acknowledge the support by the Welch Foundation grant C-1716, the National Science Foundation grant NSF CMMI 0800896, and the Air Force Research Laboratory grant AFRL FA8650-07-2-5061. The authors thank Ms. W. Gao and Prof. Pulickel Ajayan for help provided with EIS measurements, and Dr. Xin Li and Ms. Heping Shen for useful discussions and IPCE measurements

■ REFERENCES

(1) Grätzel, M. *J. Photochem. Photobiol., A* **2004**, *164*, 3.
(2) Nazeeruddin, M. K.; Angelis, F. D.; Fantacci, S.; Selloni, A.; Viscardi, G.; Liska, P.; Ito, S.; Takeru, B.; Grätzel, M. *J. Am. Chem. Soc.* **2005**, *127*, 16835.
(3) Chiba, Y.; Islam, A.; Watanabe, Y.; Komiya, R.; Koide, N.; Han, L. Y. *Jpn. J. Appl. Phys.* **2006**, *45*, L638.
(4) Nam, J. G.; Park, Y. J.; Kim, B. S.; Lee, J. S. *Scr. Mater.* **2010**, *62*, 148.
(5) Lee, K. S.; Lee, W. J.; Park, N. G.; Kim, S. O.; Park, J. H. *Chem. Commun.* **2011**, *47*, 4264.
(6) Wongcharee, K.; Meeyoo, V.; Chavadej, S. *Sol. Energy Mater Sol. Cells* **2007**, *91*, 566.
(7) Polo, A. S.; Iha, N. Y. M. *Sol. Energy Mater. Sol. Cells* **2006**, *90*, 1936.
(8) Smestad, G.; Bignozzi, C.; Argazzi, R. *Sol. Energy Mater. Sol. Cells* **1994**, *32*, 259.
(9) Imoto, K.; Takahashi, K.; Yamaguchi, T.; Komura, T.; Nakamura, J.; Murata, K. *Sol. Energy Mater. Sol. Cells* **2003**, *79*, 459.
(10) Murakami, T. N.; Ito, S.; Wang, Q.; Nazeeruddin, M. K.; Bessho, T.; Cesar, I.; Liska, P.; Humphry-Baker, R.; Comte, P.; Péchy, P.; Grätzel, M. *J. Electrochem. Soc.* **2006**, *153*, A2255.
(11) Kay, A.; Grätzel, M. *Sol. Energy Mater. Sol. Cells* **1996**, *44*, 99.
(12) Ramasamy, E.; Lee, W. J.; Lee, D. Y.; Song, J. S. *Electrochem. Commun.* **2008**, *10*, 1087.
(13) Suzuki, K.; Yamaguchi, M.; Kumagai, M.; Yanagida, S. *Chem. Lett.* **2003**, *32*, 28.
(14) Lee, S. U.; Choi, W. S.; Hong, B. *Sol. Energy Mater. Sol. Cells* **2010**, *94*, 680.
(15) Mei, X. G.; Cho, S. J.; Fan, B. H.; Ouyang, J. Y. *Nanotechnology* **2010**, *21*, 395202.
(16) Chou, C. S.; Huang, C. I.; Yang, R. Y.; Wang, C. P. *Adv. Powder Technol.* **2010**, *21*, 542.
(17) Calogero, G.; Bonaccorso, F.; MaragÒ, O. M.; Gucciardi, P. G.; Marcoa, G. D. *Dalton Trans.* **2009**, *39*, 2903.
(18) Aitola, K.; Kaskela, A.; Halme, J.; Ruiz, V.; Nasibulin, A. G.; Kauppinen, E. I.; Lunda, P. D. *J. Electrochem. Soc.* **2010**, *157*, B1831.
(19) Pint, C. L.; Pheasant, S. T.; Parra-Vasquez, A. N. G.; Horton, C.; Xu, Y. Q.; Hauge, R. H. *J.Phys. Chem. C* **2009**, *113*, 4125.
(20) Lee, C. P.; Lin, L. Y.; Chen, P. Y.; Vittala, R.; Ho, K. C. *J. Mater. Chem.* **2010**, *20*, 3619.
(21) Pint, C. L.; Xu, Y. Q.; Moghazy, S.; Cherukuri, T.; Alvarez, N. T.; Haroz, E. H.; Mahzooni, S.; Doorn, S. K.; Kono, J.; Pasquali, M.; Hauge, R. H. *ACS Nano* **2010**, *4*, 1131.
(22) Pint, C. L.; Xu, Y. Q.; Morosan, E.; Hauge, R. H. *Appl. Phys. Lett.* **2009**, *94*, 182107.
(23) Tawfick, S.; O'Brien, K.; Hart, A. J. *Small* **2009**, *5*, 2467.
(24) Pint, C. L.; Xu, Y. Q.; Pasquali, M.; Hauge, R. H. *ACS Nano* **2008**, *2*, 1871.
(25) Pint, C. L.; Nicholas, N.; Duque, J. G.; Parra-Vasquez, A. N. G.; Pasquali, M.; Hauge, R. H. *Chem. Mater.* **2009**, *21*, 1550.
(26) de Villoria, R. G.; Hart, A. J.; Wardle, B. L. *ACS Nano* **2011**, *5*, 4850.